

GPU-Resident Gaussian Process Regression Leveraging Asynchronous Tasks with HPX

Henrik Möllmann^[0009-0007-1006-5122], Dirk Pflüger^[0000-0002-4360-0212], and
Alexander Strack^[0000-0002-9939-9044]

Institute of Parallel and Distributed Systems, University of Stuttgart,
70569 Stuttgart, Germany
st178292@stud.uni-stuttgart.de
{alexander.strack, dirk.pflueger}@ipvs.uni-stuttgart.de

Abstract. Gaussian processes (GPs) are a widely used regression tool, but the cubic complexity of exact solvers limits their scalability. To address this challenge, we extend the GPRat library by incorporating a fully GPU-resident GP prediction pipeline. GPRat is an HPX-based library that combines task-based parallelism with an intuitive Python API. We implement tiled algorithms for the GP prediction using optimized CUDA libraries, thereby exploiting massive parallelism for linear algebra operations. We evaluate the optimal number of CUDA streams and compare the performance of our GPU implementation to the existing CPU-based implementation. Our results show the GPU implementation provides speedups for datasets larger than 128 training samples. We observe speedups of up to 4.3 for the Cholesky decomposition itself and 4.6 for the GP prediction. Furthermore, combining HPX with multiple CUDA streams allows GPRat to match, and for large datasets, surpass cuSOLVER’s performance by up to 11 percent.

Keywords: Gaussian Process Regression · Cholesky Decomposition · Asynchronous Many-task Runtimes · Tiled Algorithms · HPX · CUDA · GPRat

1 Introduction

The rapid advancement of artificial intelligence (AI) drives hardware development, necessitating software that can effectively utilize specialized accelerators. Consequently, existing libraries must adapt to support GPU computation to keep up with growing computational demands.

Gaussian Processes (GPs) are powerful probabilistic models used in diverse fields, ranging from AI [10] and scientific computing [22] to big data [26] and control theory [5, 23]. One key application of GPs in control theory is system identification (SI) [27], specifically for modeling non-linear dynamic systems. In this work, we consider a coupled mass-spring-damper system where the position of the last mass is non-linearly dependent on the force applied to the first mass. We employ an NFIR model, where the system state is represented by a feature

vector $\mathbf{x}_i \in \mathbb{R}^D$ containing D regressors. Using a simulator, we generate training and test datasets of input-output pairs (\mathbf{x}_i, y_i) by observing the input force and the output position at a constant rate.

The popularity of GPs is not only linked to their ability to capture non-linear relationships but also to their ability to provide uncertainty estimates. However, making exact predictions with or without uncertainty estimation requires the inversion of a large covariance matrix. This inversion can be exactly computed with the Cholesky decomposition. Thus, the cubic time complexity $\mathcal{O}(n^3)$ dominates the runtime. While libraries like GPyTorch [14] and GPflow [29] address this challenge by relying on the internal parallelization of their BLAS backend, the GPRat library [18] employs an asynchronous tiled algorithm approach using the HPX runtime system [21]. This design aims to reduce runtime and memory consumption by utilizing smaller tiles and executing sequential BLAS operations on different tiles in parallel. The goal of this work is to extend the GPRat library with support for NVIDIA GPUs to accelerate GP predictions.

The main contributions of this work include:

- Extension of the GPRat library with a fully GPU-resident GP prediction using CUDA libraries and the task-based runtime system HPX.
- Performance evaluation of the tiled Cholesky decomposition for multiple streams with HPX against the cuSOLVER reference.
- Performance comparison of the *Cholesky* and *Prediction with Full Covariance* operations between running on the CPU and GPU.

The remainder of this work is organized as follows. Section 2 provides an overview of related work. Section 3 describes the software stack used in GPRat, including HPX and the specific CPU and GPU backends. Section 4 details the methods, covering GP regression, tiled algorithms, and the specific GPU implementation. Section 5 presents the performance analysis and CPU versus GPU comparison. Finally, in Section 6 we conclude and outline future work.

2 Related Work

GPs are implemented in several Python libraries. The most popular libraries are GPyTorch [14] and GPflow [29]. GPyTorch leverages the cuSOLVER [33] or MAGMA library [2] for linear algebra, utilizing PyTorch’s dynamic computational graphs. It supports Blackbox Matrix-Matrix multiplication (BBMM) and LanczOs Variance Estimates (LOVE) [37] for scalable inference. GPflow builds on TensorFlow, benefiting from its scalability and accelerator support. Recently, GPJax [36] has emerged using the JAX [7] framework. Other libraries like scikit-learn [35] and GPy [1] offer limited or no GPU support. Their core logic is primarily written in Python, which limits their scalability compared to the C++ backends of TensorFlow and PyTorch.

To achieve maximum hardware utilization, parallel programming models are essential. Asynchronous many-task runtimes (AMTRs) have emerged as powerful tools for tackling irregular problems, such as the Cholesky decomposition. A

taxonomy of existing AMTRs is given in [41]. Several AMTRs are further compared in a recent survey by Schuchart et. al. [38]. The ExaGeoStat library [3] uses GPs for geostatistical modeling. Originally based on StarPU [4], ExaGeoStat is also compatible with PaRSEC [6,9] for better scalability.

In this work, we use the HPX library [21], which is fully compliant with the C++ standard API and supports task concatenation via futures. Applications apart from GPRat [18] include HPX-FFT [40] and the astrophysics code OctoTiger [28].

3 Software Stack

The GPRat library is built upon a robust software stack that combines the performance of C++ with the ease-of-use of Python. In this section, we present HPX, which we use for asynchronous parallelization, and the BLAS backends for CPU and GPU.

3.1 HPX

We utilize the HPX [21] runtime system for asynchronous task management. HPX provides an asynchronous task-based programming model that avoids global synchronization barriers common in fork-join models such as OpenMP [13] or message-based models such as MPI [30]. Instead, it relies on fine-grained tasks and lightweight threads. The core of GPRat’s parallelism relies on `hpx::async` and `hpx::dataflow`, which schedule tasks based on futurized data dependencies. The `hpx::dataflow` construct allows for implicit dependency management. We wrap each matrix tile in a `hpx::shared_future` object. To access the results of computations, the `get()` member function is employed, which synchronizes the execution by blocking only when a specific matrix tile is required. Consequently, this dependency-driven execution model minimizes idle time and maximizes resource utilization by effectively hiding synchronization latencies through the overlapping of computation and data access. HPX can utilize APEX [19], which allows efficient performance measurements of individual computation steps without synchronization barriers. In this work, we add support for APEX to GPRat.

3.2 CPU Backends

For the CPU backend, GPRat relies on highly optimized BLAS and LAPACK implementations. In this work, we use Intel oneMKL [20], taking advantage of its vectorized math routines. Since GPRat manages parallelism via HPX at the tile level, we configure Intel oneMKL to run sequentially to avoid oversubscription and interference between the HPX scheduler and the internal threading of Intel oneMKL. This ensures that the runtime system has full control over the distribution of work across the available cores. Note that in recent releases, GPRat also supports OpenBLAS [43] as a more portable alternative to Intel oneMKL.

3.3 GPU Backends

The GPU-resident implementation proposed in this work uses the CUDA Toolkit. Specifically, we use the cuBLAS [32] library for standard BLAS operations and the cuSOLVER [33] library for the Cholesky decomposition on individual tiles. These operations use a single CUDA stream specified in the function call. Using different streams allows operations to overlap asynchronously. Treating CUDA calls as CPU functions (distinguished primarily by a GPU context) allows for seamless integration into the HPX task graph. This maintains a unified, asynchronous execution model across the host and the device. However, both CUDA libraries expect column-major matrix ordering. This differs from the row-major layout standard in Python, C++, and consequently GPRat. To account for that difference, we introduce reformulation of the original equations. By relying on CUDA-specific libraries, our approach limits GPRat to NVIDIA accelerators. However, we plan to support more portable BLAS libraries in future releases.

4 Methods

This section details the methodologies employed in GPRat. First, we introduce the theoretical foundation of GP regression. We then describe the tiled algorithm approach, which uses independent tasks to enable asynchronous parallel execution. Finally, we discuss the GPU implementation.

4.1 Gaussian Process Regression

GPs are a probabilistic regression method used for modeling non-linear system behavior $f : \mathbb{R}^D \rightarrow \mathbb{R}, \mathbf{x} \mapsto y$ using a black-box approach [16, 23, 24]. This approach is particularly valuable when a physical derivation of the system’s dynamics is too complex or entirely unavailable. Instead of relying on explicit physical laws, the model learns the system’s behavior directly from observed input-output data. A feature vector $\mathbf{x} = [x_1, \dots, x_D] \in \mathbb{R}^D$ comprises $D \in \mathbb{N}$ features. In the context of SI, these features correspond to the D regressors formed by lagged system inputs. The output $y \in \mathbb{R}$ represents the corresponding noisy observations. GPs model this relationship probabilistically, defined as $f(\mathbf{x}) \sim \text{GP}(m(\mathbf{x}), k(\mathbf{x}_i, \mathbf{x}_j))$. For simplicity, we assume a zero mean function $m(\mathbf{x}) = 0$. The covariance function $k(\mathbf{x}_i, \mathbf{x}_j)$, also known as the kernel, measures the similarity between feature vectors. In this work, we utilize the squared exponential kernel [42]:

$$k(\mathbf{x}_i, \mathbf{x}_j) := v \cdot \exp\left(-\frac{1}{2\ell} \sum_{d=1}^D (x_{i_d} - x_{j_d})^2\right) + \delta_{i,j} \sigma^2. \quad (1)$$

This kernel depends on three hyperparameters: the lengthscale ℓ , the vertical lengthscale v , and the noise variance σ^2 . While hyperparameters are typically subject to optimization, we utilize fixed default values of $\ell = 1, v = 1, \sigma^2 = 0.1$ for the experiments presented here for simplicity.

Prediction relies on a training set with n training samples as a feature matrix $\mathbf{X} \in \mathbb{R}^{n \times D}$ and observations $\mathbf{y} \in \mathbb{R}^n$. To predict \hat{n} new observations $\hat{\mathbf{y}} \in \mathbb{R}^{\hat{n}}$ for a test feature matrix $\hat{\mathbf{X}} \in \mathbb{R}^{\hat{n} \times D}$, we have to assemble multiple covariance matrices where each entry (i, j) corresponds to the kernel evaluation $k(\mathbf{a}_i, \mathbf{b}_j)$ for feature vectors \mathbf{a}_i and \mathbf{b}_j taken from \mathbf{X} or $\hat{\mathbf{X}}$. We define the training covariance matrix $\mathbf{K} := \mathbf{K}_{\mathbf{X}, \mathbf{X}} \in \mathbb{R}^{n \times n}$, the cross-covariance matrix $\mathbf{K}_{\hat{\mathbf{X}}, \mathbf{X}} \in \mathbb{R}^{\hat{n} \times n}$, and the prior test covariance matrix $\mathbf{K}_{\hat{\mathbf{X}}, \hat{\mathbf{X}}} \in \mathbb{R}^{\hat{n} \times \hat{n}}$. The predictive mean is calculated as:

$$\hat{\mathbf{y}} := \mathbf{K}_{\hat{\mathbf{X}}, \mathbf{X}} \cdot \mathbf{K}^{-1} \cdot \mathbf{y}. \quad (2)$$

Direct inversion of \mathbf{K} is avoided to ensure numerical stability. Instead, we exploit the symmetric, positive semi-definite property of \mathbf{K} to apply the Cholesky decomposition $\mathbf{K} = \mathbf{L} \cdot \mathbf{L}^\top$, where \mathbf{L} is a lower triangular matrix. The prediction is then computed efficiently by solving $\mathbf{L} \cdot \boldsymbol{\beta} = \mathbf{y}$ (forward substitution), followed by $\mathbf{L}^\top \cdot \boldsymbol{\alpha} = \boldsymbol{\beta}$ (backward substitution), and finally $\hat{\mathbf{y}} = \mathbf{K}_{\hat{\mathbf{X}}, \mathbf{X}} \cdot \boldsymbol{\alpha}$.

Simultaneously, GPs provide uncertainty estimates via the posterior covariance matrix $\boldsymbol{\Sigma}_{\hat{\mathbf{X}}}$. While the matrix \mathbf{K} represents prior covariances based on kernel evaluations, $\boldsymbol{\Sigma}_{\hat{\mathbf{X}}}$ represents the conditional covariance after observing the training data. The diagonal elements of $\boldsymbol{\Sigma}_{\hat{\mathbf{X}}}$ represent the predictive variances, derived from:

$$\boldsymbol{\Sigma}_{\hat{\mathbf{X}}} := \mathbf{K}_{\hat{\mathbf{X}}, \hat{\mathbf{X}}} - \mathbf{K}_{\hat{\mathbf{X}}, \mathbf{X}} \cdot \mathbf{K}^{-1} \cdot \mathbf{K}_{\mathbf{X}, \hat{\mathbf{X}}}. \quad (3)$$

Computationally, this is handled by solving $\mathbf{L} \cdot \mathbf{V} = \mathbf{K}_{\mathbf{X}, \hat{\mathbf{X}}}$ for \mathbf{V} , computing the temporary matrix $\mathbf{W} := \mathbf{V}^\top \cdot \mathbf{V}$, and finally obtaining $\boldsymbol{\Sigma}_{\hat{\mathbf{X}}} = \mathbf{K}_{\hat{\mathbf{X}}, \hat{\mathbf{X}}} - \mathbf{W}$. For large test datasets, the latter steps are increasingly computationally expensive compared to the Cholesky decomposition.

4.2 Tiled Algorithms

To handle the computational complexity of GPs, specifically the cubic complexity of the Cholesky decomposition, we employ tiled algorithms. These algorithms parallelize GP operations by dividing the computation into smaller tasks distributed across multiple hardware cores. This asynchronous, task-based approach has been shown to offer superior scalability and parallel efficiency compared to standard reference implementations [39]. Our primary focus is the tiled Cholesky decomposition of the symmetric, positive semi-definite covariance matrix $\mathbf{K} \in \mathbb{R}^{n \times n}$. This tiled approach offers significant memory advantages, requiring only 50% to 75% of the memory compared to storing the entire symmetric matrix.

The matrix \mathbf{K} is split into $M \times M$ tiles $\mathbf{K}_{I,J} \in \mathbb{R}^{m \times m}$, where $m = n/M$. The tiled algorithm utilizes a *right-looking* strategy [8]. There also exist *left-* and *top-looking* variants [12]. The tiled algorithm relies on four standard BLAS operations optimized for memory access [25]:

1. **POTRF**: Cholesky decomposition on diagonal tile ($\mathbf{L}_{J,J} \leftarrow \text{Chol}(\mathbf{K}_{J,J})$).
2. **TRSM**: Solve triangular system on current column ($\mathbf{L}_{I,J} \leftarrow \mathbf{L}_{J,J}^{-1} \mathbf{K}_{I,J}$).
3. **SYRK**: Update diagonal tiles ($\mathbf{K}_{I,I} \leftarrow \mathbf{K}_{I,I} - \mathbf{L}_{I,J} \mathbf{L}_{I,J}^\top$).

```

1: for  $J \leftarrow 0$  to  $M - 1$  do
2:   POTRF( $\mathbf{K}_{J,J}$ )
3:   for  $I \leftarrow J + 1$  to  $M - 1$  do
4:     TRSM( $\mathbf{K}_{J,J}, \mathbf{K}_{I,J}$ )
5:   end for
6:   for  $I \leftarrow J + 1$  to  $M - 1$  do
7:     SYRK( $\mathbf{K}_{I,J}, \mathbf{K}_{I,I}$ )
8:     for  $K \leftarrow J + 1$  to  $I - 1$  do
9:       GEMM( $\mathbf{K}_{I,J}, \mathbf{K}_{K,J}, \mathbf{K}_{I,K}$ )
10:    end for
11:  end for
12: end for

```

Fig. 1: Tiled Cholesky decomposition of \mathbf{K} .

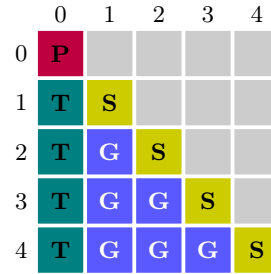


Fig. 2: Example for matrix \mathbf{K} split into 5×5 tiles, colored by tasks in the first iteration ($J = 0$): **POTRF**, **TRSM**, **SYRK**, and **GEMM**.

- GEMM**: Update off-diagonal tiles ($\mathbf{K}_{I,K} \leftarrow \mathbf{K}_{I,K} - \mathbf{L}_{I,J} \mathbf{L}_{K,J}^\top$).

Figures 1 and 2 present the algorithmic structure alongside a visualization of the matrix state during the first iteration ($J = 0$). In this step, POTRF is executed on the top-left diagonal matrix tile. Subsequently, TRSM is applied to all matrix tiles in the column below. The resulting tiles are then used to update the trailing sub-matrix via SYRK and GEMM, effectively preparing the matrix for the next iteration ($J = 1$).

4.3 GPU Implementation

In this work, we accelerate the tiled algorithms by leveraging NVIDIA GPUs. We utilize the cuBLAS [32] and cuSOLVER [33] libraries for standard linear algebra routines, while custom CUDA kernels handle GP-related tasks such as the asynchronous assembly of the covariance matrix. We prioritize minimizing data transfer overhead; therefore, we employ manual memory management rather than Unified Memory, which has been shown to incur performance penalties [31]. Both training and test datasets are explicitly copied to the device, all computations are performed entirely in device memory, and only the final results are retrieved to the host. Consequently, the tiled matrices in the GPU implementation are represented as `std::vector<hpx::shared_future<double*>>`, where each future holds a pointer to the specific matrix tile in device memory.

Regarding stream management, HPX offers executors for CUDA and cuBLAS kernels but currently lacks support for cuSOLVER. To maintain consistency across all library calls and ensure precise control over execution, we rely on CUDA streams and handles directly. GPRat initializes a user-configurable pool of CUDA streams and handles. To manage the large number of independent tasks generated by the tiled algorithms, we employ a simple round-robin scheduling strategy to assign streams to tasks. This strategy distributes operations across the available streams to facilitate concurrent execution without the substantial

overhead of creating and destroying streams for each task. Stream synchronization is handled via `cudaStreamSynchronize` directly within the HPX tasks calling cuBLAS and cuSOLVE kernels, allowing the HPX runtime to manage task dependencies via `hpx::dataflow` and ensure asynchronous execution.

Another significant challenge in integrating standard CUDA libraries with GPRat is the different memory layout. GPRat, designed for compatibility with Python and C++, utilizes row-major storage with 0-based indexing. In contrast, cuBLAS and cuSOLVER assume column-major storage with 1-based indexing. Explicitly transposing matrices in memory introduces substantial overhead. Instead, we exploit the algebraic property that a matrix \mathbf{A} stored in row-major order is identical in memory to its transpose \mathbf{A}^\top stored in column-major order. Consequently, we adapt the BLAS calls by logically transposing the matrix equations.

For example, for the TRSM operation, we transpose the defining equation to map it to column-major routines:

$$\mathbf{K}_{J,J}^\top \cdot \mathbf{L}_{I,J} = \mathbf{K}_{I,J} \quad (4)$$

$$\iff (\mathbf{K}_{J,J}^\top \cdot \mathbf{L}_{I,J})^\top = \mathbf{K}_{I,J}^\top \quad (5)$$

$$\iff \mathbf{L}_{I,J}^\top \cdot (\mathbf{K}_{J,J}^\top)^\top = \mathbf{K}_{I,J}^\top \quad (6)$$

In this transformed context, we ensure that every matrix appears transposed at least once, allowing it to be interpreted as a column-major matrix in standard BLAS routines. For instance, $(\mathbf{K}_{J,J}^\top)^\top$ represents the row-major stored $\mathbf{K}_{J,J}$ interpreted as a column-major matrix that must be transposed. Therefore, we invoke `cublasDtrsm` with the `CUBLAS_OP_T` flag. Additionally, the multiplication ordering changes, requiring the side parameter to be switched. Similar transformations are applied to SYRK and GEMM operations to ensure correct mathematical results without explicit data rearrangement. For functions involving symmetric matrices where only one triangular part is referenced (e.g., POTRF), we utilize the fact that the lower triangular part of a row-major matrix corresponds to the upper triangular part of a column-major matrix, passing `CUBLAS_FILL_MODE_UPPER` accordingly.

5 Results

In this section, we present the results of our Cholesky decomposition analysis and performance comparison between CPU and GPU. We evaluated the performance of the GPRat library on a single node equipped with a dual-socket AMD EPYC 9274F CPU with a total of 2×24 cores and theoretical peak performance of 3.1 TFLOPS and a TDP of 640W. The node also features a NVIDIA A30 GPU (24 GB) with a theoretical peak performance of 5.2 TFLOPS and a TDP of 165W. The software stack includes GPRat *v*0.3.1, HPX 1.10.0, CUDA 12.0.1, and Intel oneMKL 2024.2.2. Runtimes were averaged over 50 runs for runs shorter than 1×10^{-2} s and ten runs for longer runs. Error bars represent the 95% confidence interval.

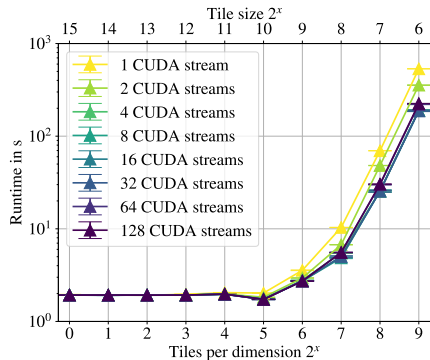


Fig. 3: Runtime of Cholesky on GPU for a problem size of $n = 32768$ with varying CUDA streams and tiles.

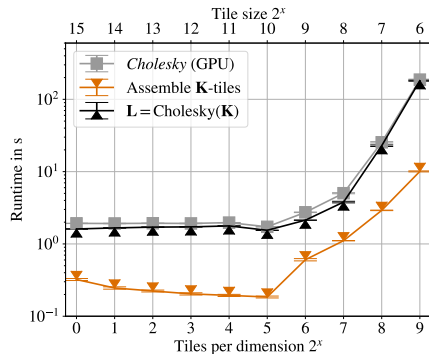


Fig. 4: Breakdown of Cholesky runtime steps on GPU for a problem size of $n = 32768$ and 32 streams with varying tiles.

5.1 Cholesky Decomposition

We analyzed the runtime of the Cholesky decomposition both on CPU and GPU. Using tiled algorithms yields the additional benefit of reduced memory consumption, as only non-empty tiles for the lower triangular factor need to be stored. In terms of CPU performance, on our 48-core test system, we observed a speedup of approximately 43.7 compared to sequential execution. Furthermore, the assembly of the covariance matrix has a quadratic time complexity $\mathcal{O}(n^2)$ and is therefore significantly faster than the Cholesky decomposition with cubic time complexity $\mathcal{O}(n^3)$. For the GPU implementation, we investigated the scalability with respect to the number of tiles and CUDA streams. Figure 3 shows that using 32 CUDA streams with 32 tiles per dimension yields the optimal performance for $n = 32768$. This configuration achieves a runtime reduction of approximately 11% compared to using a single tile. Using a single tile is equivalent to a pure cuSOLVER call, meaning our tiled approach with 32 streams outperforms using the cuSOLVER library in a direct comparison. The overhead of managing more streams or tiles outweighs the benefits of increased parallelism beyond this point. Decomposing the total runtime into its components (see Figure 4) confirms that the Cholesky factorization itself, although the dominant factor, benefits from parallelization when a specific tiling of the covariance matrix is used.

Additionally, we visualize the Cholesky decomposition using the NVIDIA Visual Profiler on a GTX 1050 GPU (see Figure 5) to show the scheduling and execution of the tiled operations on the GPU. The timeline flows from left to right and contains rectangles that represent CUDA kernel calls. Three rows are used to draw overlapping kernel calls, revealing limited concurrency, with overlap primarily at the start and end of kernel execution. Note the asynchronous scheduling of TRSM and trailing sub-matrix updates. The cuSOLVER POTRF itself applies a parallel algorithm based on tiled operations, executing multiple

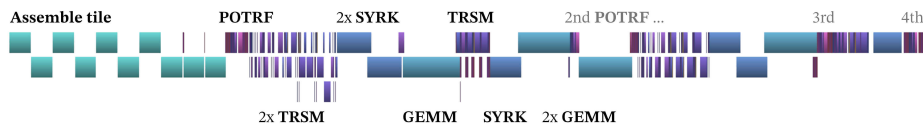


Fig. 5: Cholesky in NVIDIA Visual Profiler for $n = 4096$ training samples, four tiles, and four streams.

CUDA kernels sequentially within a single CUDA stream, where each kernel parallelizes the computation of matrix entries across GPU threads. This inherent parallelism within the kernels typically saturates GPU resources, resulting in smaller performance improvements from the HPX-based tiled algorithm compared to the CPU variant, which uses a sequential backend. The assembly kernels do not overlap. However, in Figure 4 we observe a runtime reduction for the covariance matrix assembly. This is caused by the tiled data structure of the covariance matrix, for which fewer entries have to be computed with increasing tiles.

5.2 CPU and GPU Comparison

Comparing CPU and GPU performance for *Cholesky* (see Figure 6), the GPU implementation outperforms the CPU for problem sizes $n \geq 128$. For smaller problem sizes, the sequential execution on a single tile is faster due to task management overheads in the HPX runtime. For $n = 32\,768$, the GPU implementation (with 32 tiles per dimension) achieves a speedup of approximately 4.3 over the CPU implementation (with 64 tiles per dimension). For the *Predict with Full Covariance Matrix* operation (see Figure 7), where the number of test samples \hat{n} corresponds to the number of training samples n , the GPU implementation achieves a speedup of 4.6 over the CPU version at $n = 16\,384$. Although the theoretical peak FLOPS of our test system would suggest a speedup of roughly 1.7, in practice, the GPU implementation achieves a significantly higher speedup. This is caused by CPU strong scaling limitations on our system, related to the dual-socket configuration and chiplet design of contemporary AMD CPUs [18]. Our results highlight the superiority of modern accelerators for compute-heavy workloads. In our benchmarks, the GPU delivers over four times the performance while consuming only one quarter of the energy.

6 Conclusion and Outlook

In this work, we extended the GPRat library with a fully GPU-resident GP prediction combining CUDA and HPX. The implementation of tiled algorithms for the Cholesky decomposition and prediction allows efficient distribution of tasks across the available hardware. Our results show that the GPU implementation achieves significant speedups over the CPU implementation for datasets larger than ($n \geq 128$) samples. We achieve speedups of up to 4.3 for Cholesky

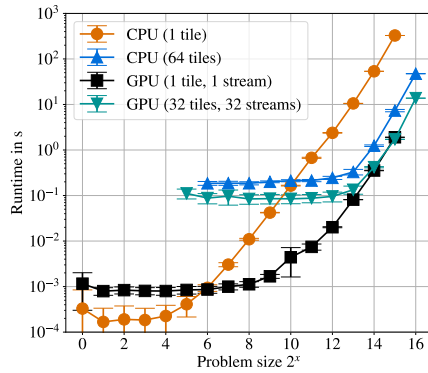


Fig. 6: *Cholesky* problem size scaling comparison between CPU and GPU.

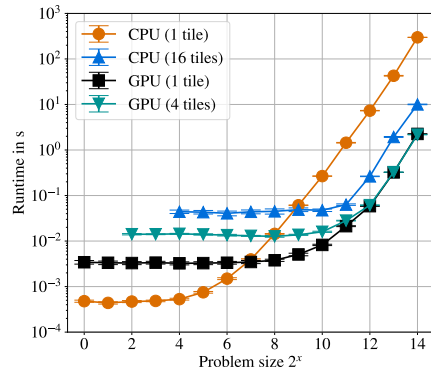


Fig. 7: *Predict Full Covariance* problem size scaling comparison between CPU and GPU.

decomposition itself and speedups of up to 4.6 for the GP prediction and uncertainty estimation. Through the use of multiple CUDA streams, our approach can beat cuSOLVER by up to 11% for the right configuration, even though we add additional task creation and scheduling overhead with the HPX runtime.

Future work will focus on optimizations to further improve the utilization of the GPU. Since distributed computing is supported by the underlying HPX runtime, we aim to extend the library to distributed multi-GPU environments to overcome single-node memory limitations. Additionally, we plan to implement heterogeneous computing to leverage both CPU and GPU resources simultaneously, ensuring maximum hardware utilization. Finally, we plan to introduce mixed-precision calculations to take advantage of modern hardware capabilities.

Supplementary Materials

The GPRat library is publicly available as open-source software under the MIT License on [GitHub](https://github.com)¹. For result reproduction, use GPRat release v0.3.1, which includes NVIDIA GPU support as well as special compilation flags to measure the runtime of individual computation steps using APEX. Datasets of arbitrary size can be generated with GPRat’s mass-spring-damper simulator. A reference dataset is available on [DaRUS](https://doi.org/10.18419/DARUS-4743)².

AI Use Disclosure

Generative AI tools, including Grammarly [17], DeepL [11], Gemini [15], and ChatGPT [34], were employed to enhance the clarity, grammar, and overall coherence of the manuscript. All technical content, data analyses, and research findings were conceived and developed independently by the authors. AI-assisted outputs were carefully

¹ <https://github.com/SC-SGS/GPRat> Accessed: 2026-01-10

² <https://doi.org/10.18419/DARUS-4743> Accessed: 2026-01-10

reviewed, verified, and edited by the authors to ensure factual accuracy, interpretive rigor, and scholarly integrity. The final manuscript reflects the authors' original intellectual contributions and analytical work.

References

1. Sheffield Machine Learning: GPY: A gaussian process framework in python. <http://github.com/SheffieldML/GPY> (2012), accessed: 2026-01-10
2. Abdelfattah, A., Beams, N., Carson, R., et al.: MAGMA: Enabling exascale performance with accelerated BLAS and LAPACK for diverse GPU architectures. *Int. J. High Perform. Comput. Appl.* **38**(5), 468–490 (2024)
3. Abdulah, S., Ltaief, H., Sun, Y., et al.: Exageostat: A high performance unified software for geostatistics on manycore systems. *IEEE Transactions on Parallel and Distributed Systems* **29**(12), 2771–2784 (2018)
4. Augonnet, C., Thibault, S., Namyst, R., et al.: StarPU: a unified platform for task scheduling on heterogeneous multicore architectures. *Concurrency and Computation: Practice and Experience* **23**(2), 187–198 (2011)
5. Berkenkamp, F., Schoellig, A.P.: Safe and robust learning control with Gaussian processes. In: 2015 European Control Conference (ECC). pp. 2496–2501 (2015)
6. Bosilca, G., Bouteiller, A., Danalis, A., et al.: Parsec: Exploiting heterogeneity to enhance scalability. *Computing in Science & Engineering* **15**(6), 36–45 (2013)
7. Bradbury, J., Frostig, R., Hawkins, P., et al.: JAX: composable transformations of Python+NumPy programs (2018), <http://github.com/google/jax>, accessed: 2026-01-10
8. Buttari, A., Langou, J., Kurzak, J., et al.: A class of parallel tiled linear algebra algorithms for multicore architectures. *Parallel Computing* **35**(1), 38–53 (2009)
9. Cao, Q., Abdulah, S., Alomairy, R., et al.: Reshaping geostatistical modeling and prediction for extreme-scale environmental applications. In: SC22: International Conference for High Performance Computing, Networking, Storage and Analysis. pp. 1–12 (2022)
10. Damianou, A., Lawrence, N.D.: Deep Gaussian processes. In: Proceedings of the Sixteenth International Conference on Artificial Intelligence and Statistics. vol. 31, pp. 207–215. PMLR, Scottsdale, Arizona, USA (29 Apr–01 May 2013)
11. DeepL SE: Deepl translator. <https://www.deepl.com/translator> (2026), accessed: 2026-01-10
12. Dorris, J., Kurzak, J., Luszczek, P., et al.: Task-Based Cholesky Decomposition on Knights Corner Using OpenMP. In: High Performance Computing. pp. 544–562. Springer International Publishing, Cham (2016)
13. Gabriel, E., Fagg, G.E., Bosilca, G., et al.: Open MPI: Goals, Concept, and Design of a Next Generation MPI Implementation. In: Recent Advances in Parallel Virtual Machine and Message Passing Interface. pp. 97–104. Springer Berlin Heidelberg, Berlin, Heidelberg (2004)
14. Gardner, J.R., Pleiss, G., Bindel, D., et al.: GPYtorch: Blackbox Matrix-Matrix Gaussian Process Inference with GPU Acceleration. In: Advances in Neural Information Processing Systems (2018)
15. Google LLC: Google gemini 3. <https://gemini.google.com/> (2026), accessed: 2026-01-10
16. Görtler, J., Kehlbeck, R., Deussen, O.: A Visual Exploration of Gaussian Processes. *Distill* (2019)

17. Grammarly, Inc.: Grammarly (version 2.0). <https://www.grammarly.com/> (2026), accessed: 2026-01-10
18. Helmann, M., Strack, A., Pflüger, D.: Gprat: Gaussian process regression with asynchronous tasks. In: *Asynchronous Many-Task Systems and Applications*. pp. 83–94. Springer Nature Switzerland, Cham (2025)
19. Huck, K.A.: Broad Performance Measurement Support for Asynchronous Multi-Tasking with APEX. In: *2022 IEEE/ACM 7th International Workshop on Extreme Scale Programming Models and Middleware (ESPM2)*. pp. 20–29 (2022)
20. Intel Corporation: Intel® oneAPI Math Kernel Library Version 2024.2.2. Intel Corporation (2024)
21. Kaiser, H., Diehl, P., Lemoine, A.S., et al.: HPX - The C++ Standard Library for Parallelism and Concurrency. *Journal of Open Source Software* **5**(53), 2352 (2020)
22. Kennedy, M.C., O’Hagan, A.: Bayesian calibration of computer models. *Journal of the Royal Statistical Society: Series B (Statistical Methodology)* **63**(3), 425–464 (2001)
23. Kocijan, J.: *Modelling and control of dynamic systems using Gaussian process models*. Springer (2016)
24. Kocijan, J., Murray-Smith, R.: Nonlinear Predictive Control with a Gaussian Process Model, pp. 185–200. Springer Berlin Heidelberg, Berlin, Heidelberg (2005)
25. Kowarschik, M., Weiß, C.: An Overview of Cache Optimization Techniques and Cache-Aware Numerical Algorithms. In: *Algorithms for Memory Hierarchies: Advanced Lectures*, pp. 213–232. Springer Berlin Heidelberg, Berlin, Heidelberg (2003)
26. Liu, H., Ong, Y.S., Shen, X., et al.: When Gaussian Process Meets Big Data: A Review of Scalable GPs. *IEEE Transactions on Neural Networks and Learning Systems* **31**(11), 4405–4423 (2020)
27. Ljung, L.: Perspectives on system identification. *Annual Reviews in Control* **34**(1), 1–12 (2010)
28. Marcelllo, D.C., Shiber, S., Marco, O.D., et al.: Octo-Tiger: a new, 3D hydrodynamic code for stellar mergers that uses HPX parallelization. *Monthly Notices of the Royal Astronomical Society* **504**(4), 5345–5382 (04 2021)
29. Matthews, A.G.d.G., van der Wilk, M., Nickson, T., et al.: GPflow: A Gaussian process library using TensorFlow. *Journal of Machine Learning Research* **18**(40), 1–6 (apr 2017)
30. Message Passing Interface Forum: MPI: A Message-Passing Interface Standard Version 5.0 (Jun 2025), <https://www.mpi-forum.org/docs/mpi-5.0/mpi50-report.pdf>, accessed: 2026-01-10
31. Nadal-Serrano, J.M., Lopez-Vallejo, M.: A performance study of cuda uvm versus manual optimizations in a real-world setup: Application to a monte carlo wave-particle event-based interaction model. *IEEE Transactions on Parallel and Distributed Systems* **27**(6), 1579–1588 (2016)
32. NVIDIA Corporation: cuBLAS Library User Guide. NVIDIA Corporation (2026), accessed: 2026-01-10
33. NVIDIA Corporation: cuSOLVER Library User Guide. NVIDIA Corporation (2026), accessed: 2026-01-10
34. OpenAI: Chatgpt 5. <https://openai.com/chatgpt> (2026), accessed: 2026-01-10
35. Pedregosa, F., Varoquaux, G., Gramfort, A., et al.: Scikit-learn: Machine Learning in Python. *J. Mach. Learn. Res.* **12**(null), 2825–2830 (Nov 2011)
36. Pinder, T., Dodd, D.: GPJax: A Gaussian Process Framework in JAX. *The Journal of Open Source Software* **7**(75), 4455 (Jul 2022)

37. Pleiss, G., Gardner, J.R., Weinberger, K.Q., et al.: Constant-time predictive distributions for gaussian processes. CoRR **abs/1803.06058** (2018)
38. Schuchart, J., Diehl, P., Bauer, M., et al.: A survey of distributed asynchronous many-task models and their applications (Dec 2025), preprint
39. Strack, A., Pflüger, D.: Scalability of Gaussian Processes Using Asynchronous Tasks: A Comparison Between HPX and PETSc. In: Asynchronous Many-Task Systems and Applications. pp. 52–64. Springer Nature Switzerland, Cham (2023)
40. Strack, A., Taylor, C., Diehl, P., et al.: Experiences porting shared and distributed applications to asynchronous tasks: A multidimensional fft case-study. In: Asynchronous Many-Task Systems and Applications. pp. 111–122. Springer Nature Switzerland, Cham (2024)
41. Thoman, P., Dichev, K., Heller, T., et al.: A taxonomy of task-based parallel programming technologies for high-performance computing. J. Supercomput. **74**(4), 1422–1434 (04 2018)
42. Williams, C.K., Rasmussen, C.E.: Gaussian processes for machine learning, vol. 2. MIT press Cambridge, MA (2006)
43. Zhang, X., Wang, Q., Zhang, Y.: OpenBLAS: An optimized blas library. <https://www.openblas.net> (2026), accessed: 2026-01-10